ASM Sc. J., 14, Special Issue 1, 2021 for ICSTSS2018, 100-107

Enhancement of Multiwall Carbon Nanotubes Electrochemical Supercapacitor Properties by Addition of Commercial Polypyrrole

Intan Syaffinazzilla Zaine[1*], Nur Amira Jaaffar[2], Kheirunnissa Ameirah Adeil[3], Nurul Nazwa Mohammad[1], Abd Hakim Hashim[4], Azmi Mohamed Yusof[5] and Nor Aimi Abdul Wahab[1]

[1]*Department of Applied Sciences, Universiti Teknologi MARA, Cawangan Pulau Pinang, Malaysia*

[2]*Faculty of Chemical Engineering Universiti Teknologi MARA, Cawangan Pulau Pinang, Malaysia*

[3]*Faculty of Applied Sciences, Universiti Teknologi MARA, Shah Alam, Selangor, Malaysia*

[4]*Advanced Materials Research Center, SIRIM Bhd, Kulim Hi-Tech Park, Kulim, Kedah, Malaysia*

[5]*Faculty of Mechanical Engineering, Universiti Teknologi MARA, Cawangan Pulau Pinang, Malaysia*

This research revealed the effect of adding up commercial polypyrrole (PPy) on morphology, molecular structure and electrochemical supercapacitor properties of multiwall carbon nanotubes (MWCNTs) film. The film was deposited through electrophoretic deposition (EPD) method. The method introduces an application of pyrocatechol violet (PV) act as a dispersant to disperse MWCNTs-PPy uniformly into deionised water. The uniform colloid was subjected to set direct current electric field to 20.7 V. The film was successfully deposited on anode electrode after 15 minutes of EPD. The morphology assessment of the film magnified at 30k shows the distribution of agglomeration of irregular spherical structure on continuous structure similar to wire. FTIR analysis indicated the PPy characteristic peaks with C=C stretching vibration in pyrrole ring, =C-H in plane vibration band and C=C bending band were preserved in MWCNTs-PPy spectra. The SO_3^- peak appeared in MWCNTs, PPy and composite spectra confirmed that PV adsorption happened on MWCNTs and PPy. The MWCNTs-PPy film has broad diffraction peak around $24° < 2\theta < 28°$ revealing the deposited film contain mixture of crystalline and amorphous nature. The film potential function as supercapacitor was further investigated by cyclic voltammetry and galvanostatic charge-discharge cycling. From the analysis, the specific capacitance, energy density, power density and energy efficiency of MWCNTs film have enhanced with the presence of PPy.

Keywords: dispersant; electrophoretic deposition; multiwall carbon nanotubes; polypyrrole; supercapacitor

I. INTRODUCTION

Supercapacitors are the electrochemical energy storage device that have diversified applications ranging from electric and hybrid vehicles (Burke *et al.*, 2014), aerospace, oil drilling (Matheson, 2016), solar energy harvesting (Hurley, 2009) as well as in high-tech textile (Abdelkader *et al.*, 2017). The electrodes materials are the key components that determine the supercapacitor's performance and capacity such as high capacitance, high power density, low resistance, long cycle life, high efficiency and also high energy density. To date there have been variety of electrode materials candidates such as metal oxide (Wu *et al.*, 2016), metal hydroxide (Li *et al.*, 2013), conducting polymer (Eftekhari *et al.*, 2017), carbon-based (Chen *et al.*, 2017) and composite (Chauhan *et al.*, 2017).

Electrodes materials selection play a major role in supercapacitor performance and among issues addressed in this area is the preparation or fabrication of the electrodes itself. To date, several methods for preparing the in-situ

*Corresponding author's e-mail: intan.zaine@uitm.edu.my

electrodes have been successfully established such as spin coating (Yadav & Kaur, 2016), chemical vapour deposition (CVD) (Dogru *et al.*, 2016) and thermal oxidation (Zhu *et al.*, 2015). However, little attention has been paid to the preparation of composite film from MWCNTs and commercial conducting polymer using electrophoretic deposition (EPD) method, perhaps due to the difficulty in achieving efficient colloid dispersion. The strong Van der Waals forces between the tubes cause critical agglomeration of CNTs. Many researchers use surface modification by harsh acid on CNTs to tackle the issue (Kar & Choudhury, 2013; Park *et. al.*, 2009; Rosca *et al.*, 2005). Unfortunately, this treatment would cause severe defects on the side wall and shortening of CNTs length (Datsyuk *et al.*, 2008).

In recent years, the use of dispersants in promoting stable dispersion of CNTs is getting popular. Some of the proven dispersants are eriochrome cyanine R (Yeling *et al.*, 2014), safranin (Shi & Zhitomirsky, 2013), methyl violet (Su & Zhitomirsky, 2013), aluminon (Ata *et al.*, 2012) and many others. Dispersant is a substance added to a suspension, usually a colloid, to obstruct the particles from approaching the close distance which dominates by attractive forces and to prevent the agglomeration of the suspension. Furthermore, dispersant helps to weaken the Van der Waals attraction, produce electrostatic repulsive force, assist solvation and form a protective coat around the particle (Kissa, 1999).

The approach described in this work is based on anodic EPD from MWCNTs-PPy suspensions in deionised water with the use of pyrocatechol violet (PV) as the dispersant. Efficient dispersion as well as EPD of MWCNTs-PPy was achievable using PV. By introducing PV as the dispersant, no acidic oxidation or other functionalisation techniques were used to disperse MWCNTs-PPy colloid efficiently. This approach was successfully preventing CNTs from degradation. The same dispersant was used for efficient dispersion of MWCNTs and PPy colloids before all the colloids were subjected to EPD. The deposited films acted as the control film. This research also reveals the influences of PPy on the morphology, molecular structure and electrochemical supercapacitor properties of MWCNTs prepared by EPD.

II. MATERIALS AND METHOD

MWCNTs (obtained from Hasrat Bestari Sdn. Bhd.) has mean outer diameter of 30-50 nm, length of 5-20 μm and purity more than 95 wt.%. PV was obtained from SIGMA meanwhile PPy with conductivity of 10-50 S cm^{-1} was obtained from ALDRICH. The other reagent, hydrochloric acid (HCl) with purity 99.5 wt.% was ordered from EMPARTA. Fresh deionised water was supplied from Elga Water Deionizers machine.

Three types of colloid were prepared which were MWCNTs, PPy and MWCNTs with PPy (MWCNTs-PPy). MWCNTs colloid were prepared by adding 0.2 g of as-received MWCNTs in 200 mL of the deionised water and sonicated for 1 hour. Later, PV was added to the colloid as dispersant and the mixture was magnetically stirred for 1 hour. Then the mixture was sonicated for another 6 hours to obtain uniform and stable MWCNTs colloid.

In order to prepare PPy colloid, 0.2 g of PPy was added to 200 mL of deionised water and sonicated for 1 hour. Then, PV was added and the mixture was sonicated for 1hour to form PPy colloid. Meanwhile, the MWCNTs-PPy colloid was prepared by adding PPy to disperse MWCNTs colloid. However, to oxidise PPy, 30 wt.% of PPy with 1 mole of HCl need to be shaken for 30 minutes. The ex-situ PPy oxidation allows the oxidation to occur in sufficient time. The purpose of oxidation is to increase conductivity. After adding PPy, the mixture was sonicated for another 1 hour to obtain uniform and stable MWCNTs-PPy colloid. The wt.% of PPy with respect to the weight of MWCNTs.

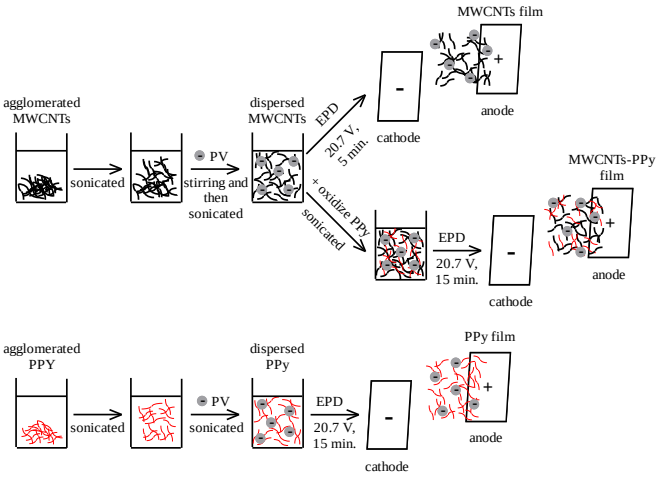

Figure 1. Fabrication of MWCNTs film, PPy film and MWCNTs-PPy film by EPD.

The colloids were then subjected to EPD procedures to produce MWCNTs film, PPy film and MWCNTs-PPy film on the nickel foil. The nickel foil was used as electrode and the distance between the electrodes was set 1 cm. After several attempts to deposit all the film, the results of the best voltage and deposition time were 20.7 V and 15 minutes, respectively. From the observation, all the films were deposited at anode. An overall step is shown in Figure 1.

The morphology and molecular structure of the films were studied using field emission scanning electron microscope (FESEM) and Fourier transform infrared spectroscopy (FTIR). Meanwhile, the structural analysis was performed using x-ray diffraction (XRD) to observe the state of deposited films.

The electrochemical supercapacitor behaviours of the films were characterised using cyclic voltammetry (CV) and galvanostatic charge-discharge (CD) cycling. The potential window used was 0.45 V and the scan rate was 2 mV s^{-1}. The electrochemical properties were conducted using three-electrode cell. The reference electrode, counter electrode and working electrode were Ag/AgCl/KCl, platinum sheet and deposited films, respectively with a geometrical area of all electrodes were 1 cm^2. All electrochemical measurements were carried out in a 6 M KOH electrolyte solution.

The CV measurement was used to evaluate the specific capacitance, C_s by using Equation (1):

$$C_s = \frac{I}{m\,S} \tag{1}$$

where I is the average current area under the graph of cyclic voltammogram, m is the mass of the working electrode and S is the scan rate. Then, the energy density, E was calculated using Equation (2):

$$E = \frac{1}{2} C_s V^2 \tag{2}$$

where V is the potential window. The CD measurement was used to evaluate the power density, P of the electrode by using Equation (3):

$$P = \frac{E}{\Delta t} \tag{3}$$

where E is the energy density and t is the discharge time in hours. Meanwhile to determine the energy efficiency, η, Equation (4) was used:

$$\eta = \frac{\text{energy from discharging}}{\text{energy from charging}} \times 100\% \tag{4}$$

III. RESULTS AND DISCUSSION

PV is polyaromatic molecules as shown in Figure 2. PV containing a SO_3^- group which is contributing to negative charge of PV. The adsorbed PV on MWCNTs will imparts a negative charge to MWCNTs. The adsorption is due to π-π interactions of the PV and MWCNTs (Wang *et. al.*, 2013; Yeling *et al.*, 2014). It provides dispersion and allowed anodic EPD. The suspension of MWCNTs, PPy and MWCNTs-PPy in DI without PV were unstable and showed fast sedimentation. The EPD for such suspensions was impossible.

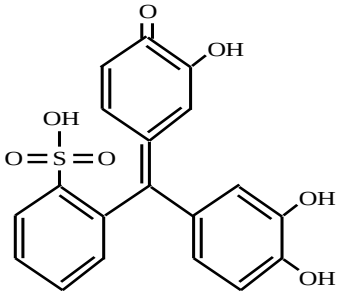

Figure 2. Chemical structure of PV

EPD by aid of PV produce smooth surface of MWCNTs film and MWCNTs-PPy film as shown in Figure 3. The films were magnified at 50. The dispersion and distribution of PPy in MWCNTs can be observed clearly at lower magnification. The dark area in Figure 3 (b) represents PPy. Although this study used DI as colloid medium, minimal pores created were observed created on the composite film. Generation of air bubbles due to hydrolysis of water lead to pore formation. This phenomenon was expected in EPD method using direct current. The micro-cracking also can be observed in white area on the composite film. It is believed due to self-aggregation of MWCNTs in the present of PPy.

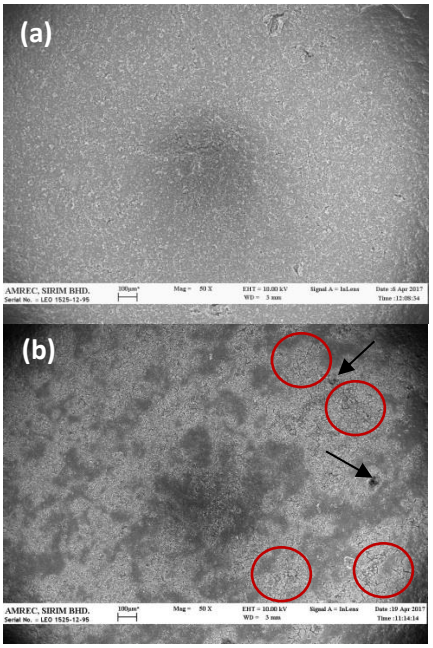

Figure 3. FESEM images magnified at 50 of (a) MWCNTs film and (b) MWCNTs-PPy film. The circles and the arrow show the cracks and the pores, respectively.

Figure 4 shows the morphology of all the films, magnified at 30 k. MWCNTs shows a continuous structure similar to wire which entangled to each other as shown in Fig. 4 (a). Fig. 4 (b) shows the irregular spherical structure of pure PPy in agglomeration form. Meanwhile, Fig. 4 (c) shows the non-uniform of PPy distribution on MWCNTs. This is probably due to the technique which adding commercial polymer, PPy, instead of adding monomer, Py during preparation of MWCNTs-PPy colloid.

Figure 5 displays the FTIR spectra of all films. FTIR spectra of pristine MWCNTs supposedly do not exhibit any significant characteristic of organic or inorganic group (Cividanes *et al.*, 2016). However, in this study, there are exist peaks at 1977 cm^{-1}, 2030 cm^{-1} and 2159 cm^{-1}. The peaks are maybe attributed to the remaining catalyst during the synthesis process. This characteristic peak is preserved in composite spectra. The adsorption peak at 1236 cm^{-1} is assigned to SO_3^- (Wang *et al.*, 2013). The peak also appeared in composite spectra at 1233 cm^{-1} and PPy spectra at 1235 cm^{-1} which confirm PV adsorption on MWCNTs and PPy. In the case of PPy spectra, the peak at 1602 cm^{-1} is associated with the C=C stretching vibration in pyrrole ring (Han *et al.*, 2014). The peak at 1496 cm^{-1} is assigned to =C-H in plane vibrations (Ruhi & Dhawan, 2014). The peak at 982 cm^{-1} is due to C=C bending band.

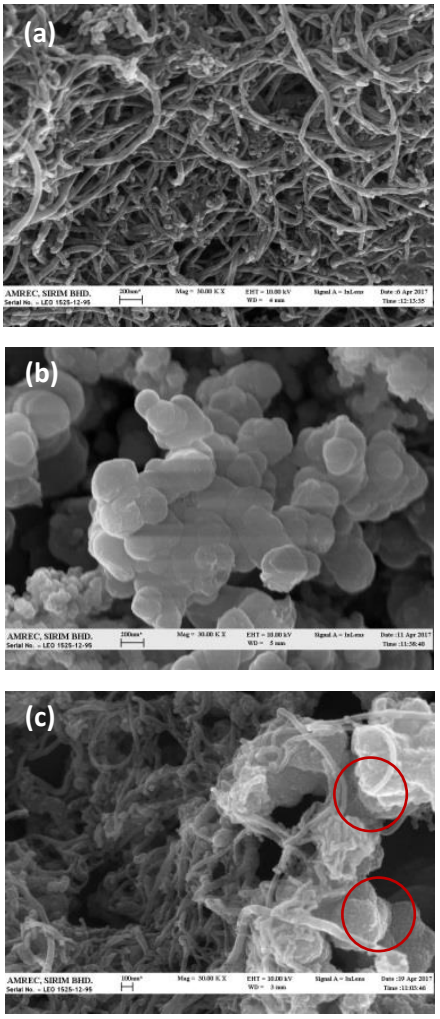

Figure 4. FESEM images magnified at 30 k of (a) MWCNTs film, (b) PPy film and (c) MWCNTs-PPy film. The circles show the PPy particles.

The composite spectra show the characteristic peak of both PPy and MWCNTs which proved that there were interactions between PPy and MWCNTs. It also confirms the presence of PPy in MWCNTs film as shown in FESEM analysis. From the spectra, it can be observed that there were shifts in all PPy characteristic peaks from higher to lower wavelength. Incorporation of PPy in MWCNTs results in shifting of the peaks which indicate the interaction of MWCNTs with different reaction sites of PPy (Imani *et al.*, 2013).

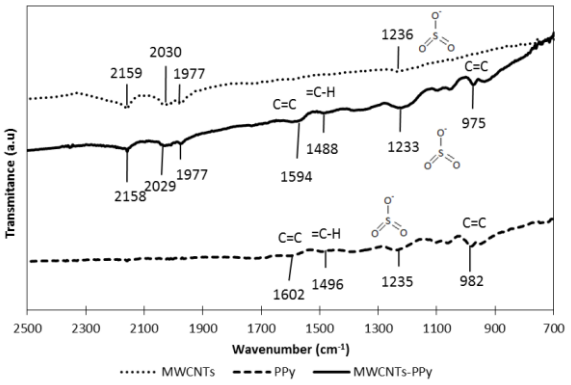

Figure 5. FTIR spectra of MWCNTs film, PPy film and MWCNTs-PPy film

Figure 6 displays the XRD pattern for all films from $10°<2\theta<40°$. The MWCNTs film show a broad and weak intense diffraction peak around $24°<2\theta<27°$ which are assigned to (002) diffraction patterns of graphite (Atchudan *et al.*, 2015). The broad peak revealing that the deposited film is not fully crystalline in nature. The PPy film also show broad peak around $24°<2\theta<28°$ which is characteristic of amorphous PPy. The peak pattern is similar as reported in literature (Chougule *et al.*, 2011). The peak is due to interplanar Van der Waals arrangement of the pyrrole-pyrrole rings in PPy chains (Li *et al.*, 2013). For composite film, the characteristics of both MWCNTs and PPy can be identified in the peak around $24°<2\theta<28°$ which match the results discovered in FESEM and FTIR analysis. XRD pattern indicates that the deposited composite film contains mixture of crystalline and amorphous nature similar with its individual component. The noise show in XRD peak was contributed by amorphous polymer.

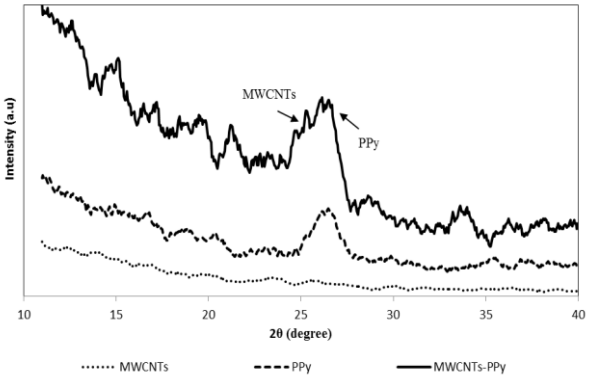

Figure 6. XRD spectra of MWCNTs film, PPy film and MWCNTs-PPy film

Figure 7 shows electrochemical changes on the film by applying potential from -0.25 V to 0.45 V at the scan rate 2 mV s^{-1}. The MWCNTs-PPy film shows the largest area of CV compared to the MWCNTs and PPy films. The larger CV area indicates higher capacitance. PPy is responsible in providing major contribution to the capacitance of MWCNTs. Obviously, the CV profiles of MWCNTs-PPy film was mainly from PPy addition since it followed the same behaviour as CV profiles of PPy film.

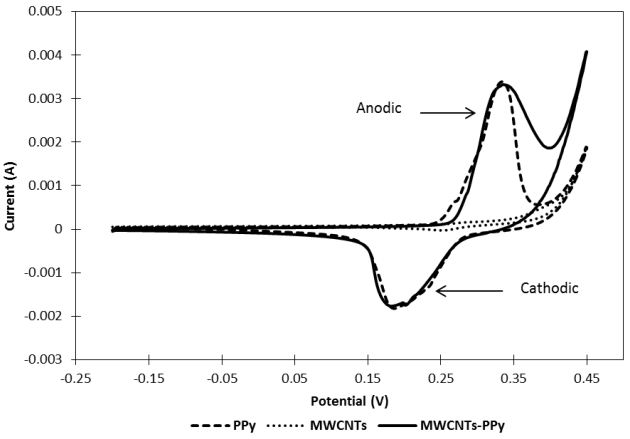

Figure 7. CV profiles of MWCNTs film, PPy film and MWCNTs-PPy film at a scan rate of 2 mV s^{-1} in 6 M KOH solution

The specific capacitance and the energy density for all films were calculated based on Figure 7 using Equation (1) and Equation (2), respectively. From the calculation, the MWCNTs-PPy film has the highest specific capacitance of 25.87 F g^{-1} which implying to the highest energy density of 2619.34 Wh kg^{-1}. The measured properties were strongly contributed from the pseudo-capacitance due to electrochemical redox reaction by PPy at the electrode-electrolyte interface. Figure 7 shows the redox reactions occur at 0.32 V and 0.19 V for both MWCNTs-PPy film and PPy film. From previous study (Ansari, 2009), the redox reaction is according to Equation (5):

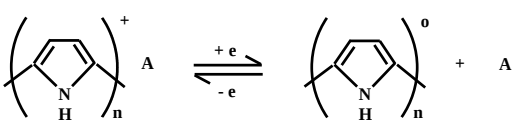

(5)

Figure 8 shows the one of the CD cycle for all films. The non-linear CD profiles for all films prove the presence of

redox reaction (Yu *et al.*, 2014). The redox reaction in MWCNTs film might be from PV or nickel current collector contribution. No significant IR drop was observed in MWCNTs-PPy film which indicates low resistance film. MWCNTs-PPy film shows the fastest and shortest charge-discharge process compared to MWCNTs and PPy films. According to Equation (3), this characteristic implying that MWCNTs-PPy film has the highest power density value which is 2619.34x10^3 W kg^{-1}.

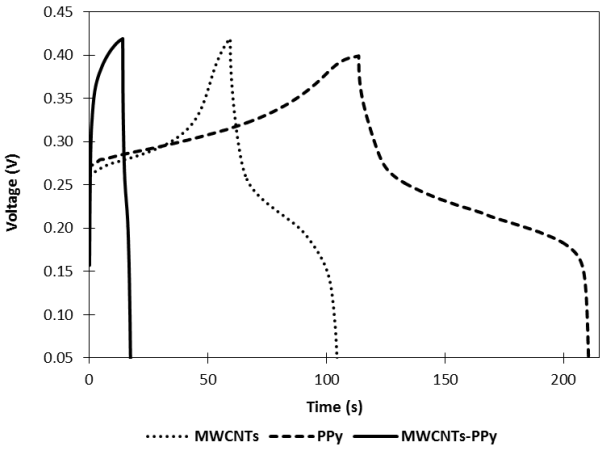

Figure 8. CD profiles of MWCNTs film, PPy film and MWCNTs-PPy film at a current density of 1 mA cm^{-2}

Figure 9 shows the energy efficiency of MWCNTs, PPy and MWCNTs-PPy films from 200 CD cycles. Energy efficiency of MWCNTs film and PPy film show dramatically drop after 30 cycles and 70 cycles respectively. After 90 cycles, energy efficiency of MWCNTs film starts to stable whereas PPy film continuously drops slowly. Meanwhile for MWCNTs-PPy film, its energy efficiency has remained constantly up to 100 cycles before slowly drops. This result suggests that the synergy between MWCNTs and PPy enhanced the stability and energy efficiency of the electrode under repeated CD cycles compared to the other films. By using Equation (4), MWCNTs-PPy film shows the highest energy efficiency which is 69.90 % although after completion of 100 cycles.

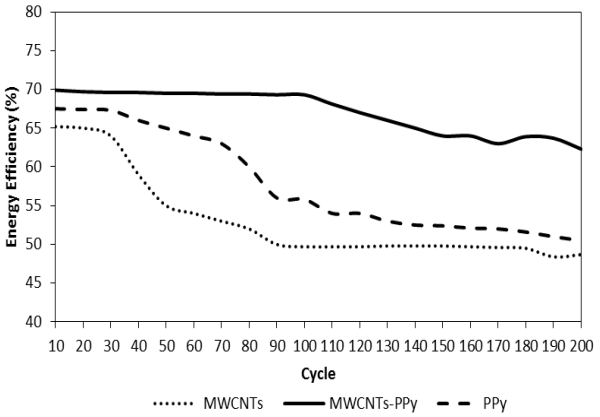

Figure 9. Energy efficiency pattern of MWCNTs film, PPy film and MWCNTs-PPy film along 200 CD cycles

Table 1 summarised all the calculated values which consist of capacitance, specific capacitance, energy density, power density and energy efficiency of all films. These values were obtained for half-cell configuration; hence it cannot be compared to Ragone plot, which stated values from full cell supercapacitor setup. Obviously, the composite film shows the best electrochemical supercapacitor properties compared to the individual films. The increment of all values was due to the present of PPy content in the MWCNTs film which contributed capacitance enhancement through redox reaction with KOH electrolyte.

Table 1. The value of capacitance, specific capacitance, energy density, power density and energy efficiency for MWCNTs film, PPy film and MWCNTs-PPy film

Properties	**MWCNTs**	**PPy**	**MWCNTs-PPy**
Capacitance (F)	0.103	0.092	0.196
Specific capacitance (F g^{-1})	7.10	18.01	25.87
Energy density (Wh kg^{-1})	718.88	1823.51	2619.34
Power density (W kg^{-1})	56.88x10^3	67.75x10^3	2619.34x10^3
Energy efficiency (%)	65.20	67.50	69.90

IV. CONCLUSION

A stable colloid of MWCNTs and PPy has been achieved prior to deposition using PV as dispersant in DI medium. The thin film MWCNTs-PPy has been successfully deposited on nickel foil using 20.7 V DC in 15 minutes. FESEM analyses show the presence of PPy on MWCNTs while FTIR analyses confirm the adsorption of PV on MWCNTs and PPy. The adsorption promoted efficient dispersion of MWCNTs and PPy throughout the EPD deposition process. XRD analysis revealed that the deposited films contain mixture of crystalline and amorphous nature. Most importantly, the CV-CD analysis of MWCNTs-PPy demonstrates good performance supercapacitor electrodes.

V. ACKNOWLEDGEMENT

The authors would like to thank the Ministry of Education, Malaysia that supports this work through Fundamental Research Grant Scheme (FRGS/1/2016/STG07/UITM/03/5).

VI. REFERENCES

Abdelkader, AM, Karim, N, Valles, C, Afroj, S, Novoselov, KS & Yeates, SG 2017, 'Ultraflexible and robust graphene supercapacitors printed on textiles for wearable electronics applications', 2D Mater., vol. 4, no. 3, pp. 35016.

Ansari, R 2009, 'In-situ cyclic voltammetry and cyclic resistometry analyses of conducting electroactive polymer membranes', Inter. J. Pharm.Tech. Res., vol. 1, no. 4, pp. 1398–1402.

Ata, MS, Sun, Y, Li, X & Zhitomirsky, I 2012, 'Electrophoretic deposition of graphene, carbon nanotubes and composites using aluminon as charging and film forming agent', Colloids Surfaces A Physicochem. Eng. Asp., vol. 398, no. Supplement C, pp. 9–16.

Atchudan, R, Pandurangan, A & Joo, J 2015, 'Effects of nanofillers on the thermo-mechanical properties and chemical resistivity of epoxy nanocomposites', J. Nanosci. Nanotechnol., vol. 15, no. 6, pp. 4255–67.

Burke, A, Liu, Z & Zhao, H 2014, 'Present and future applications of supercapacitors in electric and hybrid vehicles', in IEEE International Electric Vehicle Conference (IEVC), Florence, 17-19 December 2014, Italy.

Chauhan, H, Singh, MK, Kumar, P, Hashmi, SA & Deka, S 2017 'Development of SnS2 /RGO nanosheet composite for cost-effective aqueous hybrid supercapacitors', Nanotech., vol. 28, no. 2, pp. 25401.

Chen, X, Paul, R & Dai, L 2017, 'Carbon-based supercapacitors for efficient energy storage', Natl. Sci. Rev., pp. 1–37.

Chougule, MA, Pawar, SG, Godse, PR, Mulik, RN, Sen, S & Patil, VB 2011, 'Synthesis and characterisation of polypyrrole (PPy) thin films', Soft. Nanosci. Lett., vol. 1, no. 1, pp. 6–10.

Cividanes, LS, Thim, GP, Ferreira, FV, Brito, FS, Menezes, BRC, Franceschi, W & Simonetti, EAN 2016, Functionalizing Graphene and Carbon Nanotubes - A Review. Springer Nature.

Datsyuk, Y, Kalyva, M, Papagelis, K, Parthenios, J, Tasis, D, Siokou, A, Kallitsis, I & Galiotis, C 2008, 'Chemical oxidation of multiwalled carbon nanotubes', Carbon N. Y., vol. 46, no. 6, pp. 833–840.

Dogru, IB, Durukan, MB, Turel, O & Unalan, HE 2016, 'Flexible supercapacitor electrodes with vertically aligned carbon nanotubes grown on aluminum foils', Prog. Nat. Sci. Mater. Int., vol. 26, no. 3, pp. 232–236.

Eftekhari, A, Li, L & Yang, Y 2017, 'Polyaniline supercapacitors', J. Power Sources, vol. 347, pp. 86–107.

Han, G, Liu, Y, Kan, E, Tang, J & Zhang, L 2014, 'Sandwich-structured MnO2/polypyrrole/reduced graphene oxide hybrid composites for high-performance supercapcitors', RSC Adv., vol. 4, no. June 2015, pp. 9898–9904.

Hurley, P 2009, 'Solar supercapacitor applications', Wheelock Mountain Publications, USA.

Imani, A, Farzi, G & Ltaief, A 2013, 'Facile synthesis and characterisation of polypyrrole-multiwalled carbon nanotubes by in situ oxidative polymerisation', Int. Nano Lett., vol. 3, no. 1, pp.1- 8.

Kar, P & Choudhury, A 2013, 'Carboxylic acid functionalised multi-walled carbon nanotube doped polyaniline for chloroform sensors', Sensors Actuators, B Chem., vol. 183, pp. 25–33.

Kissa, E 1999, 'Dispersions : Characterisation, Testing and Measurement', 1st edn, Marcel Dekker Incorporation, New York, US.

Li, HB, Yu, MH, Wang, FX, Liu, P, Liang, Y, Xiao, J, Wang,

CX, Tong, YX & Yang, GW 2013, 'Amorphous nickel hydroxide nanospheres with ultrahigh capacitance and energy density as electrochemical pseudocapacitor materials', Nat. Commun., vol. 4, no. May, pp. 1-7.

Li, M, Li, W, Liu, J & Yao, J 2013, 'Preparation and characterisation of PPy doped with different anionic surfactants', Polym. Eng. Sci., vol. 53, no. 11, pp. 2465–2469.

Li, Y 2015, 'Organic optoelectronic materials', Org. Optoelectron. Mater., pp. 27–33.

Matheson, R 2016, New applications for ultracapacitors, MIT News, viewed 10 July 2018, <http://energy.mit.edu/news/new-applications-ultracapacitors/>.

Park, OK, Jeevananda, T, Kim, NH, Kim, S & Lee, JH 2009, 'Effects of surface modification on the dispersion and electrical conductivity of carbon nanotube/polyaniline composites', Scr. Mater., vol. 60, no. 7, pp. 551–554.

Rosca, ID, Watari, F, Uo, M & Akasaka, T 2005, 'Oxidation of multiwalled carbon nanotubes by nitric acid', Carbon N. Y., vol. 43, no. 15, pp. 3124–3131.

Ruhi, G & Dhawan, SK 2014, 'Conducting polymer nano composite epoxy coatings for anticorrosive applications', Mod. Electrochem. Methods Nano, Surf. Corros. Sci., pp. 99-137.

Shi, K & Zhitomirsky, I 2013, 'Electrophoretic nanotechnology of graphene-carbon nanotube and graphene-polypyrrole nanofiber composites for electrochemical supercapacitors', J. Colloid Interface Sci., vol. 407, pp. 474–81.

Su, Y & Zhitomirsky, I 2013, 'Electrophoretic deposition of graphene, carbon nanotubes and composite films using methyl violet dye as a dispersing agent', Colloids Surfaces A Physicochem. Eng. Asp., vol. 436, no. Supplement C, pp. 97–103.

Wang, Y, Liu, Y & Zhitomirsky, I 2013, 'Surface modification of MnO2 and carbon nanotubes using organic dyes for nanotechnology of electrochemical supercapacitors', J. Mater. Chem. A, vol. 1, no. 40, pp. 12519.

Wu, Z, Zhu, Y, Ji, X & Banks, CE 2016, 'Transition metal oxides as supercapacitor materials,' Nanomaterials in Advanced Batteries and Supercapacitors, K. I. Ozoemena and S. Chen, Eds. Cham: Springer International Publishing, pp. 317–344.

Yadav, S & Kaur, I 2016, 'Low temperature processed graphene thin film transparent electrodes for supercapacitor applications', RSC Adv., vol. 6, no. 82, pp. 78702–78713.

Yeling, Z, Kaiyuan, S & Zhitomirsky, I 2014, 'Anionic dopant-dispersants for synthesis of polypyrrole coated carbon nanotubes and fabrication of supercapacitor electrodes with high active mass loading', J. Mater. Chem. A, vol. 2, no. 35, pp. 14666–14673.

Yu, W, Jiang, X, Ding, S & Li, BQ 2014, 'Preparation and electrochemical characteristics of porous hollow spheres of NiO nanosheets as electrodes of supercapacitors', J. Power Sources, vol. 256, pp. 440–448.

Zhu, S, Dai, Y, Huang, W, Zhang, C, Zhao, Y, Tan, L & Wang, Z 2015, 'In situ preparation of NiO nanoflakes on Ni foams for high performance supercapacitors', Mater. Lett., vol. 161, pp. 731–734.